RSC Advances

ROYAL SOCIETY OF CHEMISTRY

www.rsc.org/advances

Investigation of Morphological and Characterization of Rare earth metal Samarium hexacyanoferrate and its composite with surfactant intercalated graphene oxide for sensor application

Balamurugan Devadas, Srikanth Cheemalapati, Shen-Ming Chen* Muniyandi Rajkumar

Electroanalysis and Bio electrochemistry Laboratory,

Department of Chemical Engineering and Biotechnology,

National Taipei University of Technology,

No.1, Section 3, Chung-Hsiao East Road, Taipei 106,

Taiwan (ROC).

*Corresponding author

*E-mail: smchen78@ms15.hinet.net

Tel: (886)-2-27017147, Fax: (886) -2-27025238.

Abstract

Herein, we report a facile electrochemical approach for the hierarchical growth of samarium hexacyanoferrate (SmHCF) on surfactant intercalated reduced graphene oxide (SRGO). The fabricated SRGO/SmHCF modified glassy carbon electrode (GCE) has excellent electrocatalytic activity towards catechol (CC) sensor application. The sunflower like SmHCF micro particle was achieved by controlling the number of cycles during electrodeposition process. In addition, the electrolyte plays a key role in the morphologies of SmHCF and was investigated using different electrochemical techniques. The as-prepared SmHCF micro particles were characterized by scanning electron microscopy (SEM), energy dispersive x-ray (EDX) and Fourier transform infrared (FT-IR) spectroscopy techniques. Besides, electrochemical impedance spectroscopy (EIS) studies were carried out, to understand the mechanism of interfacial electrochemical reactions on the proposed SmHCF modified glassy carbon electrode (GCE). The obtained EIS data confirmed that the electron transfer rate at SmHCF/GCE was faster than bare GCE. The electrochemical detection of CC at SRGO/SmHCF modified GCE was performed by cyclic voltammetry and difference pulse voltammetry. The fabricated modified GCE exhibits a good linear range from 50 µM to 250 µM, with a detection limit (LOD) of 0.38 µM and sensitivity was obtained as 0.430 $\mu A \mu M^{-1}$ cm^2 for CC electrochemical sensor.

Keywords: Samarium hexacyanoferrate, surfactant intercalated reduced graphene oxide, Glassy carbon electrode, catechol, electrochemical impedance spectroscopy.

1. Introduction

Metal hexacyanoferrates (MHCFs) preparation, characterization and electrochemical works were pioneered by Neff and Itaya et al. [1, 2] MHCFs are consider to be a class of poly-nuclear inorganic mixed valence compounds, zeolitic materials, showing redox and ionic conductivity properties [3, 4]. Owing to its high stability of the metal cyanide framework and cation exchanging properties, beneficial for widespread applications such as electro-chromism, electrocatalysis, electro analytical applications[5], solid state batteries[6-8] and photo image formation [9, 10]. So far several reports for the transition metal hexacyanoferrate preparation and their applications towards electro catalysis [11-13]. Nevertheless, rare-earth MHCFs have been studied in the past few decades [14], due to their special properties and which have been received great attention for the applications of batteries, sensor fields [15, 16] and electrocatalytic hydrogenation of alkenes [17].

The novel synthesis of nanostructured materials with different morphologies were recently attracted in scientific community[18], the finite size effects of the prepared nanomaterials have unusual properties and utilized in the electrical, optical and magnetic devices[19]. On the other hand, recent years various rare earth MHCFs with different morphologies were reported by electrochemical methods, such as flower like and Christmas tree like cerium hexacyanoferrate (CeHCF) [20], Carambolalike and flower like Holmium hexacyanoferrate (HoHCF)[21] and our previous reported work micro star like Dysprosium hexacyanoferrate (DyHCF)[22]. In general, all lanthanide elements have high charge density and high affinity,[23] thus it form complex with ferricyanide which results in metal hexacyanoferrate (MHCFs) formation. Herein, we successfully achieved samarium hexacyanoferrate modified electrode by electrodeposition method using ferricyanide solution containing $Sm^{3+}$with different electrolyte. Thus the SmHCF showing excellent electron transfer ability for the electrochemical sensor[24]. In addition, there are few reports were available for the SmHCF preparation and characterizations by Ping Wu et al [3,25], demonstrated an electrodeposition approach for the SmHCF at different electrolyte conditions, but specified morphology of the SmHCF is still not reported obviously. Hence, it is required to investigate the different morphologies and electrochemical behaviors of different rare earth MHCFs to develop novel kinds of electrochemical sensors [26, 27].

Being a versatile dispersant, graphene oxide (GO) has a unique properties such as exceptional ability to form stable aqueous dispersions and superior electrocatalytic properties. Due to its unique properties it was considered as a gifted materials for biological applications[28]. Hence, these fascinating and unique properties of GO has been attracted significantly in the emerging electrochemical field. In our study organic surfactant cetyl-trimethyl ammonium bromide (CTAB) was intercalated with GO (SGO) and subsequent reduction was achieved (SRGO). The SRGO, exhibits good dispersion in aqueous solvents and further it stabilizes the wrinkled structure of the graphene sheets at the time of reduction, enhances the specific capacitance [29].

Catechol (CC, 1, 2-dihydroxybenzene) is a phenolic compound and an isomer of dihydroxy-benzene,[30] widely used for pesticides, flavoring agents, medicines, dyes and antioxidant chemicals [31] respectively. According to the US Environmental Protection Agency (EPA) and the European Union (EU), CC was considered as an environmental pollutant and included in the list of priority pollutant monitoring list [32, 33]. Moreover, increase in concentration at certain level of CC in environment could be very harmful to the people, animals, plant and aquatic life [34]. Especially pesticide, tanning industrial effluents and sanitary waste water contains higher CC levels [30]. Therefore, it is an important to develop a highly sensitive analytical method to monitor the CC levels in the samples. So far, numerous methods have been developed for the CC detection, such as spectro-photometry[35], high-performance liquid chromatographic technique[36], fluorescence[37], chemiluminescence [38,] gas chromatography/ mass-spectrometry [39] and capillary electrophoresis[40]. Contrast to aforementioned technique, electrochemical method has the advantages of low cost, good response and high sensitivity.

This present work, a facile electrochemical route for the preparation of SmHCF having sunflower like structure on the surfactant intercalated reduced graphene oxide (SRGO) modified GCE for CC sensor has been reported. The SRGO/SmHCF composite, combining the individual properties of GO (large surface area and high conductivity) together with SmHCF (high recognition, thermal stability, chemical inertness, and lack of toxicity) could be an excellent approach for catechol detection. The morphologies of the SmHCF have been investigated by SEM and the fabricated SmHCF electrode was characterized by Fourier transform Infra-red (FT-IR) and energy dispersive x-ray (EDX) spectroscopy. The electrochemical characteristics of the SmHCF modified electrode was studied by electrochemical impedance spectroscopy (EIS) techniques. To the best of our understanding, the sunflowers like SmHCF morphology structures have not been reported yet. To our knowledge, reports on SmHCF preparation, characterizations and electrochemical studies are limited to a few preliminary reported works in recent years [3, 25, 27].

2. Experimental

2.1 Materials and Methods

Graphite powder, Samarium (III) chloride hexahydrate [$SmCl_3.6H_2O$] (>99%) were purchased from sigma Aldrich and used as received. Potassium Ferricyanide [$K_3Fe(CN)_6$], Potassium Chloride (KCl) and Lithium Chloride (LiCl) were purchased from wako pure chemical industries, Ltd. Sodium chloride was obtained from J.T Baker (Phillipsburg, USA). Catechol was procured from Sigma Aldrich and used as without purification. Cetyl trimethyl-ammonium bromide (CTAB) was obtained from Janssen chemicals. Doubly distilled (DD) water has been utilized for preparing the working solution. Nitrogen gas was purged throughout the electrochemical cell for few minutes prior to the electrodeposition process.

Electrochemical deposition process was performed by cyclic voltammogram (CV) technique using a CHI 1205 A electrochemical analyzer. A conventional electrochemical cell consists of three-electrode system. Glassy carbon electrode (GCE) (surface area = 0.075 cm^2) as the working electrode, Ag/AgCl (saturated KCl) as reference electrode and a platinum wire as counter electrode respectively.The potentials of all experimental results were referred to standard Ag/AgCl (saturated KCl) reference electrode. Surface characterization was studied by Scanning Electron Microscope (Hitachi, Japan). Electrochemical impedance studies (EIS) were performed by using ZAHNER impedance analyzer (ZAHNER Elektrik Gmbh & Co KG, Germany). X-ray diffraction, ultra violet spectroscopy and Infra-red spectroscopy instruments were used for the characterization studies.

2.2 Preparation SRGO/SmHCF sunflowers modified glassy carbon electrode (GCE):

The preparation procedure for graphene oxide (GO) was followed by hummer's method. Briefly, the raw graphite powder was converted into graphite oxide by treating with a mixture of concentrated sulfuric acid, sodium nitrate and potassium permanganate under the condition of hummer's procedure. Finally the obtained brown color graphite oxide was exfoliated through continuous ultra-sonication in water for 2 hr to get GO. Finally the GO was centrifuged for 15 min to remove the un-exfoliated graphite oxide. To prepare the surfactant intercalated graphene oxide (SGO), 10 ml of as prepared GO solution was added to 10 ml of 0.1M CTAB in a flask.

This reaction mixture was vigorously stirred for 72 hr, at ambient temperature. After three days, the SGO was filtered and dried at room temperature. The powder was re-dispersed in water (1 mg/ml), sonicated for 2 hours to get uniform dispersion. Then 5 µl of this dispersion was drop casted on GCE and dried at room temperature. The SGO was electrochemically reduced to SRGO using 0.1M KCl (pH 5) between the scan 0 and -1.5 V at the scan rate of 50 mV s^{-1} for 10 cycles.

The SmHCF modified SRGO/GCE was prepared by electrodeposition method using CV technique. As fabricated, SRGO/GCE was placed in an electrochemical cell, which containing freshly prepared 5 mM of $SmCl_3.6H_2O$ and $K_3Fe\ (CN)_6$ in 0.2M KCl electrolyte. 20 consecutive cyclic voltammogram scans were performed between the potential range 0.8 and -0.2 V at a scan rate of 50 mV s^{-1} (explained detail in the section 3.1). The flower like SmHCF particle was electrochemically deposited on SRGO modified GCE. Then the SmHCF modified SRGO/GCE was rinsed with water and dried at room temperature. Thus the fabricated GCE was applied for further electrochemical studies.

3. Result and Discussion

3.1 Electrochemical deposition of SmHCF micro flowers on GCE and SRGO/GCE

Electrochemical deposition of metal hexacyanoferrate using supporting electrolyte solution containing of K^+ cation, shows a well-defined reversible cyclic voltammogram (CV) and in this work we prepared SmHCF using electrolyte as KCl solution. Fig 1 depicts the CV of electrodeposition of SmHCF micro sunflower in KCl solution and the electrolyte containing equal concentration of (5mM) of $SmCl_3.6H_2O$ and $K_3Fe\ (CN)_6$ respectively. Here it can be seen that, cathodic peak appears at 0.255 V, indicating corresponding reduction of $K_3Fe\ (CN)_6^{3-}$ and the anodic peak appears at 0.3 V, reveals that characteristic oxidation of $K_3Fe\ (CN)_6^{4-}$

respectively. As expected the redox couple is progressively decreased with increase of the cycle scan. Similarly the redox couple appeared whereas deposition process of SmHCF on SRGO/GCE. The two redox couple appeared in Fig 1B, corresponds to the growing of SmHCF on SRGO/GCE. While the moment of reduction reaction occurred, the Sm^{3+} ions reacted with $K_3Fe\ (CN)_6^{4-}$ to form SmHCF micro flower particle. SRGO with negatively charged functional groups (such as carboxyl, carbonyl and epoxy) and surfactant as a supporting material that allow effective anchoring and adsorption of positively charge Sm^{3+} ions that consequently adsorbed the negatively charged HCF particles, which stabilized the as-formed SmHCF particles on the SRGO surface. As expected, relative to the deposition of SmHCF on the surface of a bare GCE, that on the SRGO surface occurred efficiently, due to the large surface area of SRGO and improved anchoring of SmHCF particles on the SRGO surface (Fig. 1B). The petal like structures of SmHCF allows them to anchor strongly on SRGO, which minimized the dissolution of the SmHCF particles. The following reaction 1 & 2 expressed the formation mechanism of SmHCF.

$$Fe\ (CN)_6^{3-} + e^- \rightarrow Fe\ (CN)_6^{4-}\text{---------------------} \ (1)$$

$$Fe\ (CN)_6^{4-} + Sm^{3+} + K^+ \rightarrow KSmFe\ (CN)_6 \text{-------------} \ (2)$$

Here, an equal amount of (5mM) Sm^{3+} and hexacyanoferrate has been taken for balanced deposition of SmHCF micro flowers. Moreover high concentration of Sm^{3+} and $K_3Fe\ (CN)_6$ were required for an effective formation of SmHCF micro flowers. In case of the lower concentration (1mM to 4 mM), the SmHCF particle does not form effectively. On the other hand, the SmHCF electrochemical deposition has been compared using different cation Na^+ and Li^+ containing electrolyte solutions. As expected, the redox peak corresponding to Na^+ and Li^+ appears at same potential of K^+ electrolyte solution [Figure not shown]. Moreover, the obtained redox peak currents and the analytical procedures were similar with that of KCl electrolyte solution studies. According to the obtained results, electrolytes containing cation does not affect the formation of SmHCF particle on GCE. Nevertheless, morphological changes occurred owing to cationic properties of electrolyte (explained in section 3.2.2).

3.2 Scanning Electron Microscopy

3.2.1 Morphologies of as prepared SRGO/SmHCF composite

The surface morphologies of as prepared SGO and SRGO/SmHCF composite were characterized using scanning electron microscopy. Figure 2A shows the surface of as prepared SGO. It can be seen that highly surfactant loaded GO looking of flaky sheets. As shown in figure 2B, the SmHCF with flower like structure formed on the surface of SRGO. The flower like SmHCF particle evenly distributed on SRGO surface and it clearly revealing that the composite of SRGO/SmHCF was formed.

3.2.2 Morphological Effect on different electrolyte

Morphologies of SmHCF in different cation (K^+, Na^+ and Li^+) containing electrolytes were investigated. Figure 3 shows different kind of surface morphology in various electrolyte. As shown in Fig 3 A, B and C, KSmHCF exhibits flower like shape, NaSmHCF exhibits butterfly like structure, and sheet like morphology for LiSmHCF. These morphological changes are mainly attributed to monovalent cations. Owing to the charge and atomic number of cation increases are causes to increasing the affinity in the order of $Li^+ < H^+ < Na^+ < K^+$. Moreover, the formal potential for the metal hexacyanoferrate always depends on the monovalent cations used in the electrolyte. However, the ionic radii differ for each electrolyte and this may leads to change the morphologies of SmHCF [41, 42].

3.2.3 Morphology changes at different cycles

The growth of SmHCF micro flower structure was carefully monitored over the period of 5th, 10th, 15th and 20th cycles respectively. Figure 4 displays the clear insights of SmHCF micro flower blooming under optimized conditions. As displayed in fig 4A, the apparent hexagonal flower bud shape with average size of 3 ± 4μM was formed at the ending of 5th cycle. Further increasing the cycle number up to 10 and 15 cycle may leads to the formation of encapsulated flower bud like structure as shown in figure 4B and 4C. This reveals that, the flowering becomes thrive (similar with unfolding stalk from the flower bud). Moreover the size of this structure became wider than flower bud. At the end of 20th cycle, the flower grew to larger sizes as displayed in figure 4D. Here, we indicate that the intrinsic smooth SmHCF sunflower (inset figure 4D) like morphologies was strongly anchored on the electrode surface. This surface morphology illustrates structure of SmHCFcomplex relative to the balanced combination between Sm^{3+} and $Fe\,(CN)_6{}^{3-}$.

3.3 Characterization

Thus prepared SmHCF micro flower was confirmed by EDX and FTIR spectroscopic characterization studies. Figure 5A displays the EDX spectra of SmHCF. It can be seen that SmHCF modified electrode contains the entire element with valid proportion. Figure 5B shows the weight % of element present in SmHCF complex. EDX profile of SmHCF exhibits 28 weight % of samarium, 9 % of Fe and 7.6% of potassium. The oxygen content indicating moisture absorbed on the SmHCF complex. On the other hand Figure 5 C shows the typical FTIR spectrum of SmHCF samples. A highly intensive peak appeared at around 2065.5 cm^{-1}, indicating presence of C≡N stretching vibration group corresponding to the hexacyanoferrate complex of SmHCF. There are two reasonable peaks at 1596. 5 and 1654.7 cm^{-1} validates binding vibration of crystal water present in SmHCF. The above results confirmed the SmHCF complex formation.

3.4 Electrochemical Impedance spectroscopy (EIS)

EIS study is one of the promising choices to elucidate the electrocatalytic behavior of the modified electrode. The figure 6A shows the Nyquist plots of the a) KSmHCF, b) NaSmHCF and c) LiSmHCF respectively. Among the various Randles equivalent circuit parameters (inset), charge transfer resistance (R_{ct}) is the valuable parameter to understand the redox reaction on electrode surface. As shown in figure 6A, the KSmHCF modified GCE having extremely small semicircle relative to other modified GCE such as NaSmHCF, LiSmHCF. The semicircle electron transfer R_{ct} values were calculated as 210, 230, and 250 Ω corresponding to KSmHCF, NaSmHCF, and LiSmHCF respectively. The lowest R_{ct} value of KSmHCF attributed to the lower electron transfer resistant (highly electron transfer ability) and good conductivity. Hence we concluded that K^+ containing electrolyte enhanced the electron transfer rate at the MHCF complex and surface of the electrode than the other two cationic electrolytes (Na^+ and Li^+). As per R_{ct} value, the NaSmHCF electron transfer resistant lies in the middle of the two MHCF complexes. So the SmHCF modified GCE electrode reaction is alkali metal cations dependent reaction [42]. The electrocatalytic behavior of SmHCF can be sorted by the following order.

KSmHCF>NaSmHCF>LiSmHCF

Electrocatalytic activity of SmHCF modified electrode was controlled by number of deposition cycles. Figure 6B shows the Nyquist plot of SmHCF modified electrode at 5, 10 and 20 cycles. The largest semi-circle with higher R_{ct} value was observed for SmHCF modified GCE at 5 cycles, indicating electron transferring process rate was leisurely and also extremely sluggish electrocatalytic behavior. Interestingly, the semicircle portion of the SmHCF modified GCE large scale decreased at 10 cycles. Compared with SmHCF modified GCE in 5 cycles, the SmHCF in 10 cycle's exhibits smaller value with R_{ct} value of 350. This result reveals that fast electron transfer process occurred on SmHCF/GCE at 10th cycles. The enormous difference of this R_{ct} value is mainly attributed to size of SmHCF increase sharply. However, exceedingly lowest semicircle value was observed at SmHCF modified GCE in 15 and 20 cycles. The R_{ct} value of SmHCF/GCE in both 15 and 20 cycles was remains similar value (figure not shown). Hence we conclud that SmHCF/GCE exhibit rapid electron transfer process at the 20 cycles. It is worth noting that, the optimum cycle deposition of SmHCFmodified GCE was carried for electrochemical oxidation reaction. As shown in Fig s1 the KSmHCF/GCE has lower electron transfer value than bare GCE. The aforementioned results validates the SmHCF has lower charge transfer resistant value at 20 CVs cycles in KCl electrolyte.

3.5 Cyclic voltammogram of SRGO/SmHCF modified GCE

Figure 7A shows the CV of a) SRGO/SmHCF/GCE b) RGO/SmHCF/GCE c) SmHCF/GCE in deoxygenated 0.1M KCl at scan rate of 50 mV s^{-1}. The highly stable enhanced redox peak was observed on SRGO/SmHCF/GCE, suggests that SmHCF particle strongly attached on the surface of SRGO/GCE. But without surfactant on GO, the deposition of SmHCF on RGO not stable as much as with compared to GO with surfactant. Though the SmHCF strongly deposited directly on GCE, which does not show any obvious redox peak relative to SRGO/SmHCF modified electrode. This result was attributed to the intercalation of surfactant on graphene sheets are improve the wettability of the electrode. Hence SmHCF strongly interact with surfactant present in graphene sheets and formed SRGO/SmHCF modified GCE.

3.6 Electrochemical determination of catechol (CC)

In order to find better and sensitive electrochemical determination of CC, the different modified electrode was employed in 0.1M KCl solution containing 0.3mM of CC using Cyclic voltammetric method at scan rate of 50 mV/s. To discern the electrochemical behavior of as synthesized GO, the GO modified GCE (without SmHCF) was employed directly for CV measurement. The Fig s2 shows the CV response of GO/GCE in presence of CC. As shown in Fig S2 the extremely poor CC oxidation response was found at +0.35 V. At the same time, the CC oxidation response was monitored with different modified electrode. Figure 7B depicts the CVs response of **0.3 mM** CC at different modified electrodes SRGO/SmHCF/GCE (a), RGO/SmHCF (b), SmHCF/GCE (c) and bare GCE (d) in deoxygenated 0.1M KCl at the scan rate of 50 mV s^{-1}. SRGO/SmHCF/GCE exhibits well defined enhanced catechol oxidation peak at +0.350 V. While compared with the other modified electrodes such as RGO/SmHCF and bare GCE, the proposed modified SRGO/SmHCF/GCE showed less positive potential for the oxidation of CC. Besides, compared with GO/GCE, the fabricated electrode exhibits enormous amount of high response for CC. Therefore, the surfactant intercalated GO and on deposited SmHCF has highly efficient than GO modified GCE. Moreover, the oxidation peak current noted at SRGO/SmHCF/GCE was higher than that of RGO/SmHCF, SmHCF and bare GCE. Hence, the CC detection at SRGO/SmHCF/GCE showing enhanced anodic current than the other electrodes which have discussed above and this method could be used to detect CC in industrial effluents and in environmental monitoring laboratories in near future.

3.7 Differential Pulse Voltammetry

Fig 8 shows the DPV response of CC at SRGO/SmHCF/GCE in 0.1M KCl at scan rate of 50 mV s^{-1}. It can be seen that the linear increasing of oxidation peak was observed with each additions of CC. The inset figure indicates, that the linear calibration plot for the concentration vs current. The linear regression equation can be expressed as I (µA) = 0.0343 C (µM) + 0.54, R^2 = 0.9755. The linear range of the CC was obtained ranging from 50 µM to 550 µM. The low limit of detection was found as 0.38 µM. The sensitivity of the SRGO/SmHCF/GCE film towards CC senor is found to be 0.430 (µAµM^{-1} cm^2). These obtained results suggest that, the fabricated GCE has excellent catalytic activity towards CC and could be used as an electrochemical sensor for CC determination in near future. We have compared the reported sensor results with other reported methods. As shown in the Table 1, the fabricated electrode has low limit of detection with other previous reported methods,

Table 1

Comparison table of catechol senor at SRGO/SmHCF/GCE with other reported methods.

S.NO	Modified electrode [a]	Linear range	LOD	Reference
1	SRGO/SmHCF/GCE	50 - 250	0.38	This work
2	Palygorskite/CPE	5 - 100	0.57	1
3	Tyrosinase	60 - 800	6	2
4	PPy/CNT/Tyrosinase	3 - 50	0.671	3
5	Tyrosinase/SPE	-	1.7	4
6	GCE in micellar solution	0.5 - 900	0.6	5
7	MWCNT/GCE	20 - 1200	10	6
8	G/Chitosan/GCE	1 - 400	0.75	7
9	MWCNT/PPy/HRP/Au	1.6 - 8	0.93	8
10	PASA/MWCNT/GCE	6 - 180	1	9

11	PPABA/GCE	2 - 900	0.5	10

[a] CPE - Carbon paste electrode, PPy – Polypyrrole, CNT – Carbon nanotube, SPE – Screen printed electrode, MWCNT – Multi walled carbon nanotube, G – Graphene, HRP -horseradish peroxidase, PASA - poly-amidosulfonic acid, PPABA - Poly(p-aminobenzoic acid).

4. Conclusion

A novel composite of SRGO/SmHCF modified GCE has been developed for CC determination using electrochemical methods. The morphologies change for SmHCF was observed in different electrolytes and cycles using SEM. The electrochemical impedance spectroscopy of SmHCF at different electrolytes and cycles have been studied. In addition, the SRGO/SmHCF/GCE has showed an excellent electro catalytic activity towards the catechol determination.

Acknowledgement

This work was supported by Ministry of science and technology, Taiwan (ROC).

References:

1 V.D. Neff, *J. Electrochem. Soc*, 1978, **125,** 886.

2 K. Itaya, T. Ataka, S. Toshima, *J. Am. Chem. Soc*., 1982, **104,** 3751.

3 P. Wu, S. Lu, C. Cai, *J. Electroanal. Chem*., 2004, **569**, 143-150.

4 S. S. Narayanan and F. Scholz, *Electroanal*, 1999, **11**, 465-469.

5 K. Itaya, I. Uchida, V.D. Neff, *Acc. Chem. Res*., 1986, **19**, 162

6 M. Kaneko, T. Okada *J. Electroanal. Chem*, 1988, **255**, 45.

7 S. Kalwellis-Mohn, E. W. Grabner, *Electrochim Acta*, 1989, **34**, 1265.

8 M. Jayalakshmi, F. Scholz, *J Power Sources*, 2000, **91**, 217

9 M. Nishizawa, S. Kuwabata, H. Yoneyama, *J. Electrochem. Soc*., 1996, **143**, 3462.

10 Y. Wu, B. W. Pfenning, A. B. Bocarsly, *InorgChem,* 1995, **34,** 4262.

11 A.P. Baionia, M. Vidottia, P.A. Fiorito, S.I. Cordoba de Torresi, *J. Electroanal. Chem.*, 2008, **622**, 219-224.

12 X. Cui, L. Hong, X. Lin, *J. Electroanal. Chem.*, 2002, **526**, 115-124

13 S.M.Chen, *J. Electroanal. Chem*, 2002, **521**, 29-52

14 D.F. Mullica, H.O. Perkins, E.L. Sappenfield, D.A. Grossie, *J. Solid State Chem.*, 1988, **74**, 9.

15 J.J.G. Willems, *Philips J. Res.*, 1984, **39**, 1.

16 S. Zhao, J.K.O. Sin, B. Xu, M. Zhao, Z. Peng, H. Cai, Sens.Actuat. B, 2000, 64, 83.

17 G.M.R.V. DrutenLabbe, V.P. Boncour, J. Perichon, G.A. Percheron. *J. Electroanal.Chem.*, 2000, **487**, 31.

18 Z. Wang, *Adv.mater.*, 2003, **15,** 432-436.

19 Y. Shi, B. Zhou, P. Wu, K. Wang, C. Cai *J. Electroanal. Chem*, 2007, **611**, 1–9.

20 L. D. Feng,M. M. Gu,Y. L. Yang, G. X. Liang, J. R. Zhang,J. J. Zhu, *J. Phys. Chem. C*, 2009 **113**, 8743–8749.

21 Y. Sun, W. Zhou, D. Zhao, J. Chen, X. Li, L. Feng, *Int. J. Electrochem. Sci,* 2012 **7**, 7555 – 7566.

22 Rajkumar, B. Devadas, S. M. Chen, *Electrochimica Acta*, 2013, **105**, 439–446.

23 M. R. Ganjali, Z. Memari, F. Faridbod, P.Norouzi*, Int. J. Electrochem. Sci.*, 2008, **3**, 1169 – 1179

24 Y. Liu, Z. Yang, Y. Zhong, J. Yu, *Applied Surface Science*, 2010, **256**, 3148–3154.

25 P. Wu, C. X. Cai., *J. Electroanal. Chem*, 2005, **576**, 49–56.

26 Q.L. Sheng, H. Yu and J. B. Zheng, *J Solid State Electrochem.,* 12, **2008**, 1077–1084

27 P. Wu, C. X. Cai, *J Solid State Eletrochem*, 2004, **8**, 538–543.

28 C. Chung, Y. K. Kim, D. Shin, S. R. Ryoo, B. H. Hong, D. H. Min, *Accounts of chemical research*, 2013, **46**, 2211–2224.

29 K. Zhang, L. Mao, L. L. Zhang, H. S. O. Chan, X. S. Zhao, J. Wu, *J. Mater. Chem.,* 2011, **21,** 7302

30 W. Liu, L. Wu, X. Zhang, and J. Chen, *Bull. Korean Chem. Soc*. 2014, **35,** 204-210

31 A. J. S. Ahammad, M. M. Rahman, G. R. Xu, S. Kim, and J. J. Lee, *Electrochimica Acta,* 2011, **56**, 5266.

32 S. R. Nambiar, P. K. Aneesh and T. P. Rao, *Analyst,* 2013, **138**, 5031-5038.

33 A. J. S. Ahammad, S. Sarker, M. A. Rahman, and J. J. Lee, *Electroanal,* 2010, **22**, 694.

34 C. Wang, R. Yuan, Y. Chai, F. Hu, Anal. Methods., 2012, 4, 1626–1628.

35 Y. C. Fiamegos, C. D. Stalikas, G. A. Pilidis and M. I. Karayannis, *Anal. Chim. Acta,* 2000, **403**, 315–323.

36 H. Cui, C. He and G. Zhao, *J. Chromatogr., A*, 1999, **855**, 171– 179.

37 M. F. Pistonesi, M. S. D. Nezio, M. E. Centurion, M. E. Palomeque, A. G. Lista, and B. S. F. Band, *Talanta,* 2006, **69**, 1265.

38 L. Zhao, B. Lv, H. Yuan, Z. Zhou, and D. Xiao, *Sensors.*, 2007, **7**, 578.

39 S. C. Moldoveanu, M. J. Kiser, *J. Chromatogr. A*, 2007, **1141**, 90.

40 M. J. Schoning, M. Jacobs, A. Muck, D. T, Knobbe, J. Wang, M. Chatrathi, S. Spillmann, *Sensor. Actuat. B-Chem*. 2005, **108**, 688.

41 Application of ion exchange processes for the treatment of radioactive waste andmanagement of spent ion exchangers - Vienna : *International AtomicEnergy Agency*, 2002,

42 I. Markovich, D. Mandler, *J. Electroanal. Chem*, 2000, **484**, 194–202.

43 Y. Konga, X. Chena, W. Wanga, Z. Chen, *Anal. Chim. Acta*, 2011, **688**, 203–207

44 S. Tembe, S. Inamdar, S. Harama, M. Karve, S.F. D. Souza, *Journal of Biotechnology*, 2007, **128**, 80–85.

45 S. K. Ozoner, M. Yalvac, E. Erhan, *Current Applied Physics*, 2010, **10**, 323–328.

46 R. Solna, S. Sapelnikova, P. Skladal, M. Winther-Nielsen,C. Carlsson, J. Emneus, T. Ruzgas, *Talanta*, 2005, **65**, 349–357.

47 J. Peng . Z. N. Gao, *Anal Bioanal Chem*, 2006, **384**, 1525–1532.

48 Z. Xu, X. Chen, X. Qu, S. Dong, *Electroanal.* 2004, **16**, 685-687.

49 H. Yina, Q. Zhang, Y. Zhoud, Q. Maa, T. liu, L. Zhu, S. Ai, Electrochim. Acta, 2011, **56**, 2748–2753.

50 S. Korkut, B. Keskinler, E. Erhan, Talanta, 2008, **76**, 1147–1152.

51 D. M. Zhao, X.H. Zhang, L.J. Feng, L. Jia, S.F. Wang, *Coll. and Sur. B: Biointerfaces,* 2009, **74**, 317–321.

52 P. Yang, Q. Zhu, Y. Chen, F. Wang, J. App. Polymer Science, 2009, **113**, 2881 – 2886.

Figure captions

Figure 1: CV deposition of SmHCF on A) GCE, B) SRGO modified GCE from 0.1M KCl containing 5 mM of $SmCl_3$ and $K_3Fe(CN)_6$ at scan rate of 50 mV/s. (20 cycles).

Figure 2: SEM image of A) SRGO B) Electrodeposited SmHCF on SRGO from 0.1M KCl containing 5 mM of $SmCl_3$ and $K_3Fe(CN)_6$ at scan rate of 50 mV/s (20 cycles).

Figure 3: SEM image of electrodeposited SmHCF at different supporting electrolyte under the condition of 0.1M electrolyte concentration. (20 cycles at scan rate of 50 mV/s A) KCl B) NaCl C) LiCl.

Figure 4: SEM images of SmHCF at different cyclic voltammetric cycles A) 5 cycles B) 10 cycles C) 15 cycles D) 20 cycles from 0.1M KCl containing 5mM of $SmCl_3$ and $K_3Fe(CN)_6$ at scan rate of 50 mV/s.

Figure 5: A) EDX elemental analysis of SmHCF B) Chart of Weight percentage (%) of different elements in SmHCF C) Infra-red spectra of SmHCF.

Figure 6: EIS of SmHCF deposition A) at different electrolytes NaCl, KCl and NaCl under the deposition condition of 20 CV cycles at the scan rate of 50 mV/s. B) at different cycles 5, 10 and 20 cycles using 0.1M KCl electrolyte containing $K_3Fe(CN)_6$ at the measured frequency from 100 mHz to 100 KHz.

Figure 7: A) CVs of various film a) SRGO/SmHCF/GCE b) RGO/SmHCF/GCE and c) SmHCF/GCE in 0.1M KCl solution at scan rate of 50 mV/s. B) CVs of SRGO/SmHCF/GCE (a), RGO/SmHCF (b), SmHCF/GCE (c) and bare GCE (d) in 0.3mM of catechol in deoxygenated 0.1M KCl at the scan rate of 50 mV s^{-1}

Figure 8: DPV of SRGO/SmHCF/GCE in various concentration of Catechol (50 to 550 µM) in 0.1M KCl solution.

Figures

Figure 1.

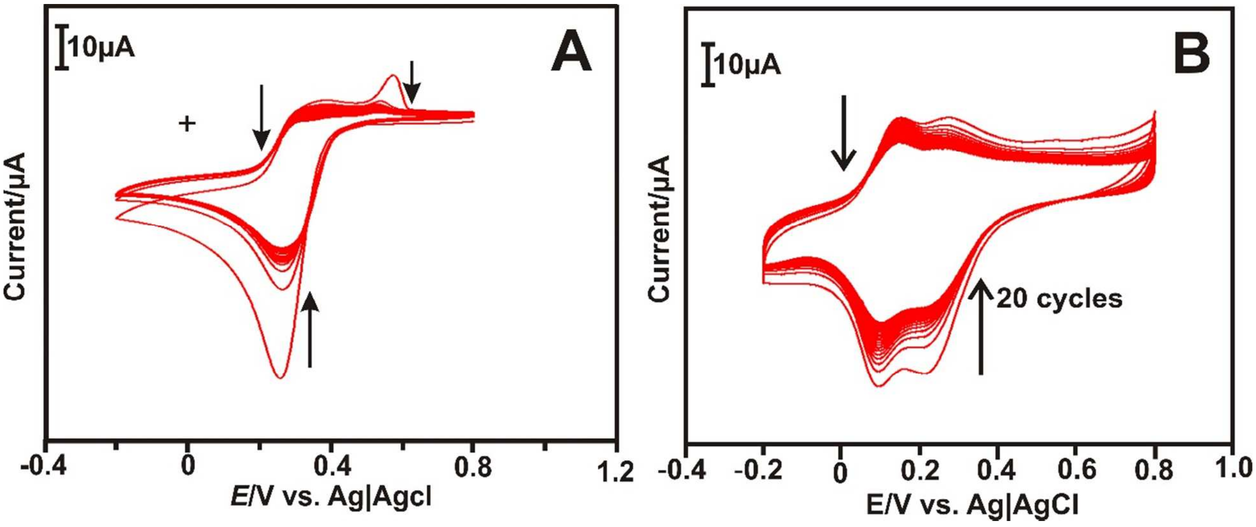

Figure 2.

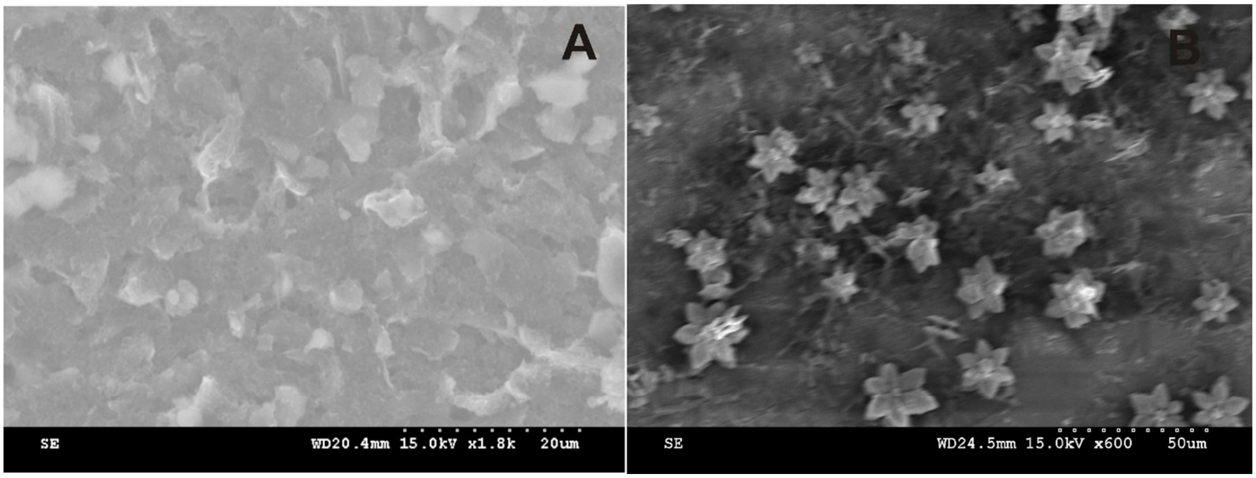

Figure 3

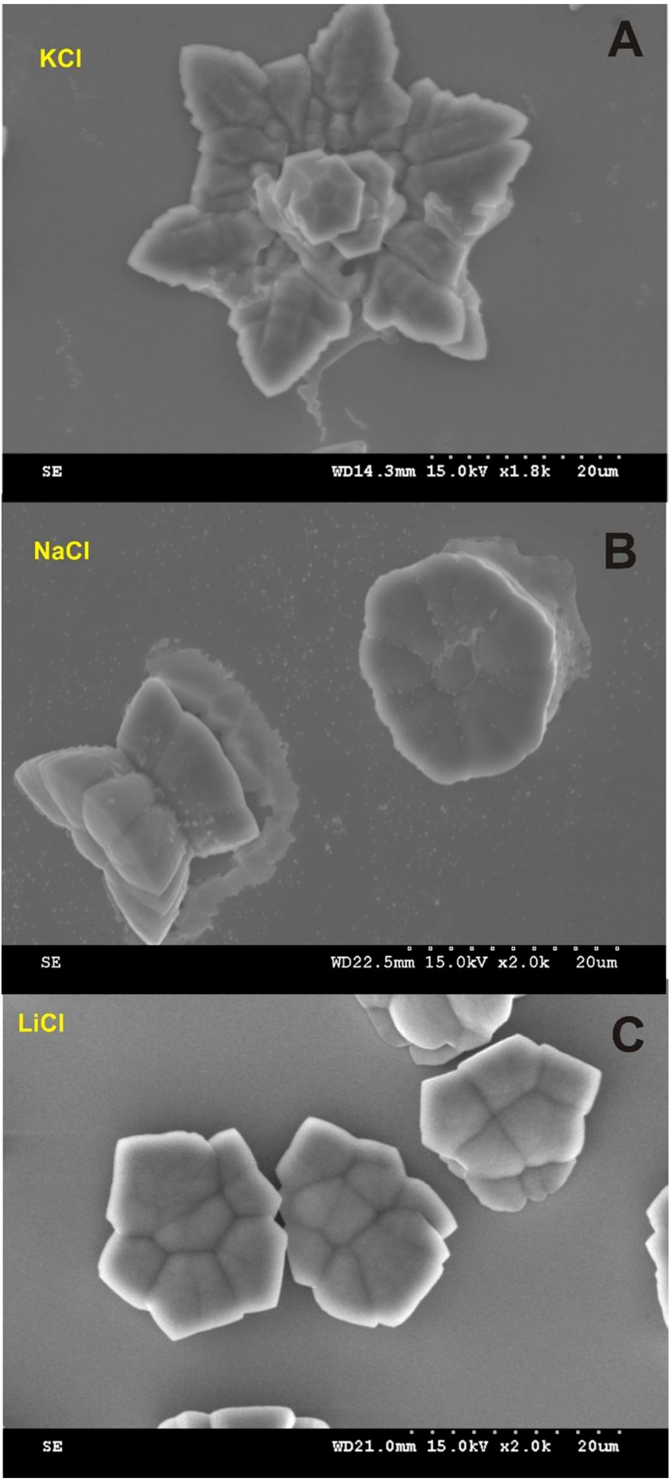
KCl
A
SE
WD14.3mm 15.0kV x1.8k 20um
NaCl
B
SE
WD22.5mm 15.0kV x2.0k 20um
LiCl
C
SE
WD21.0mm 15.0kV x2.0k 20um

Figure 4

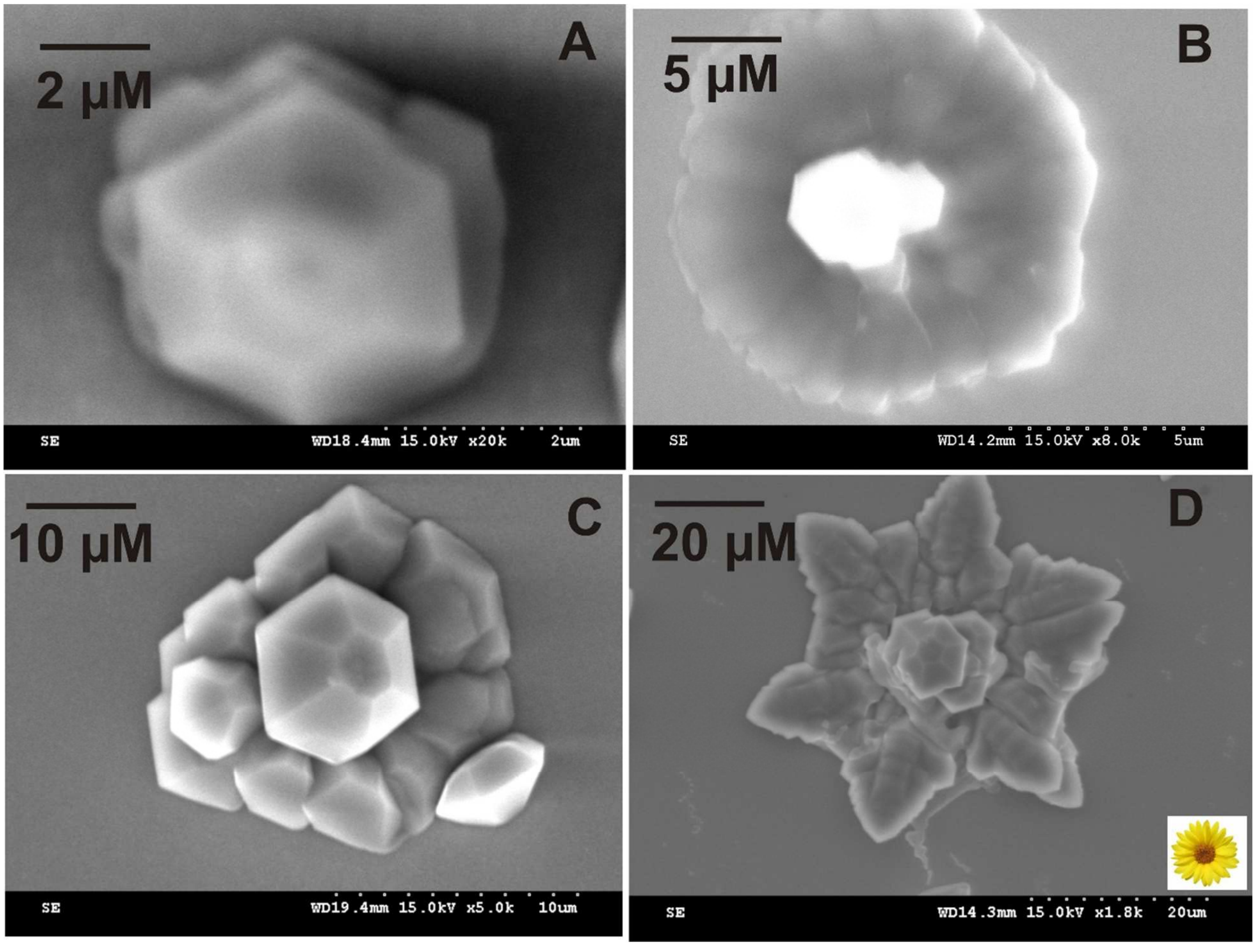
2 μM
A
SE WD18.4mm 15.0kV x20k 2um
5 μM
B
SE WD14.2mm 15.0kV x8.0k 5um
10 μM
C
SE WD19.4mm 15.0kV x5.0k 10um
20 μM
D
SE WD14.3mm 15.0kV x1.8k 20um

Figure 5

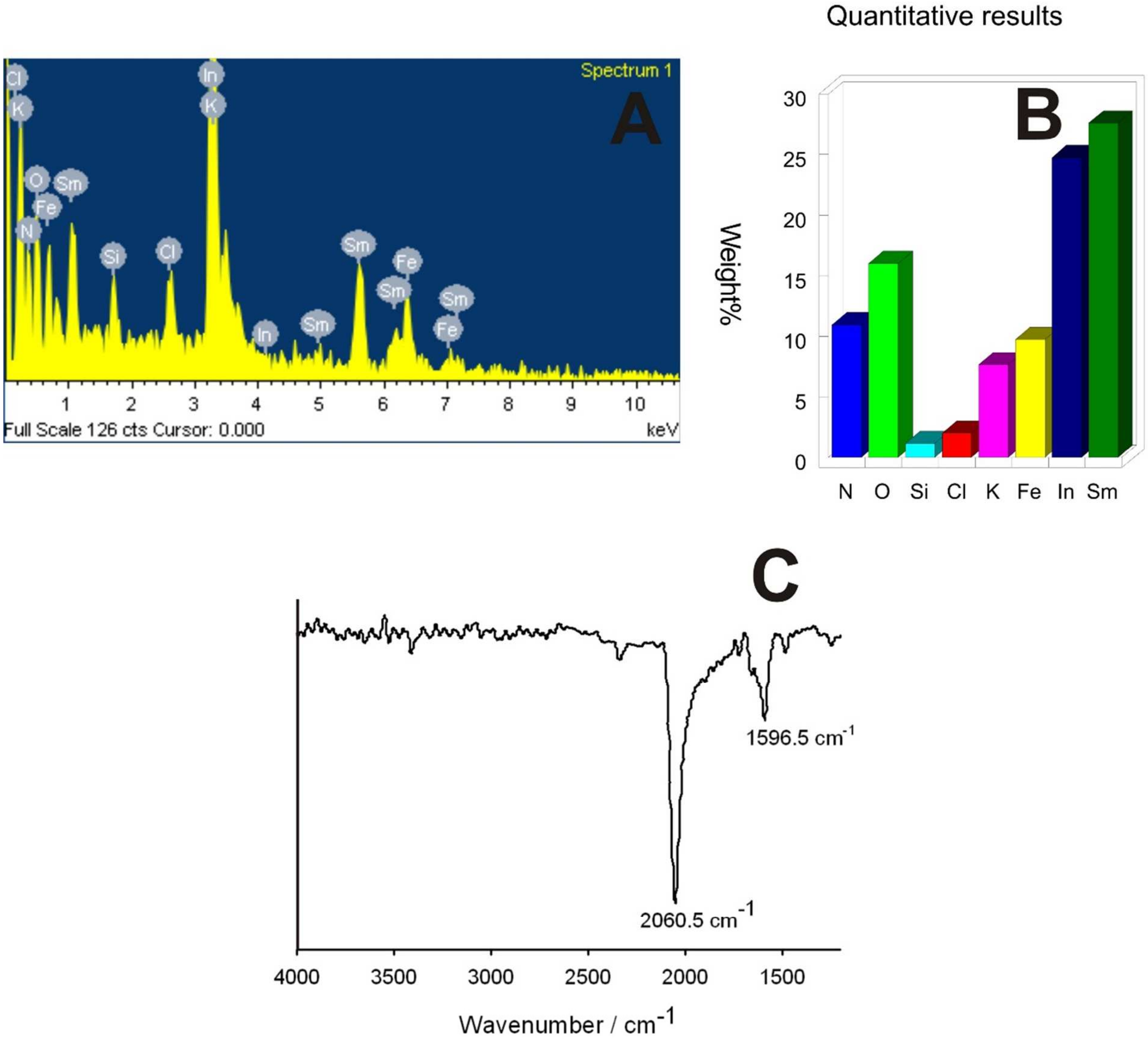
A
Spectrum 1
Cl
K
In
K
O
Sm
Fe
N
Si
Cl
Sm
Fe
Sm
Sm
In
Sm
Fe
1 2 3 4 5 6 7 8 9 10
Full Scale 126 cts Cursor: 0.000
keV
Quantitative results
B
Weight%
0 5 10 15 20 25 30
N O Si Cl K Fe In Sm
C
1596.5 cm^{-1}
2060.5 cm^{-1}
4000 3500 3000 2500 2000 1500
Wavenumber / cm^{-1}

Figure 6.

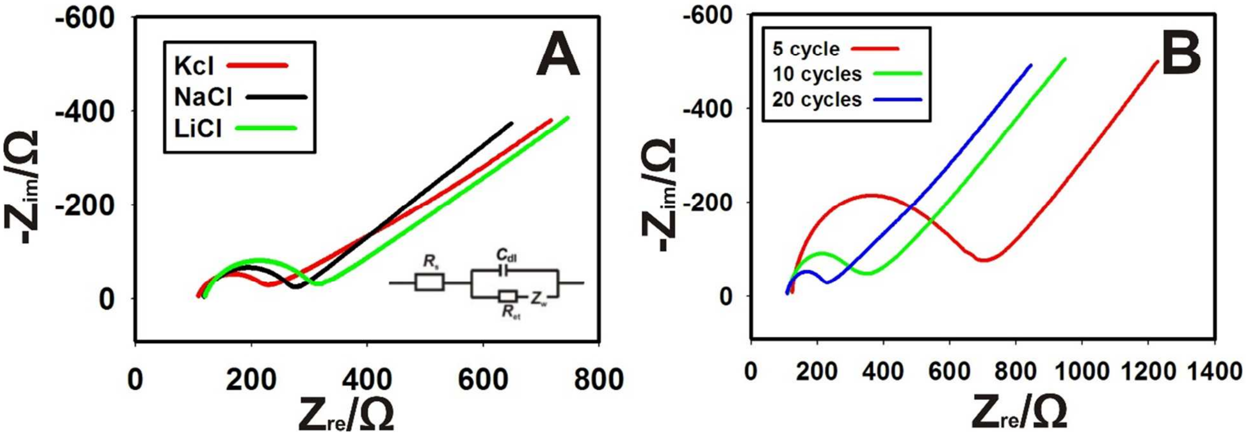
A
Kcl
NaCl
LiCl
R_s
C_{dl}
R_{ct}
Z_w
-600
-400
-200
0
0
200
400
600
800
$-Z_{im}/\Omega$
Z_{re}/Ω
B
5 cycle
10 cycles
20 cycles
-600
-400
-200
0
0
200
400
600
800
1000
1200
1400
$-Z_{im}/\Omega$
Z_{re}/Ω

Figure 7.

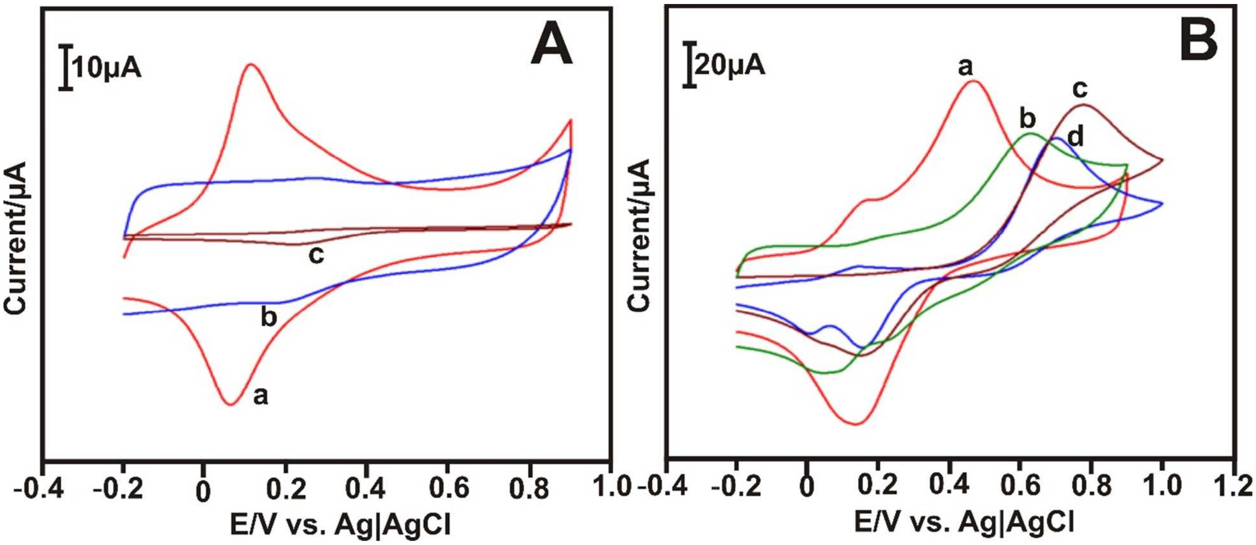
A
10μA
Current/μA
a
b
c
-0.4
-0.2
0
0.2
0.4
0.6
0.8
1.0
E/V vs. Ag|AgCl
B
20μA
Current/μA
a
b
c
d
-0.4
-0.2
0
0.2
0.4
0.6
0.8
1.0
1.2
E/V vs. Ag|AgCl

Figure 8

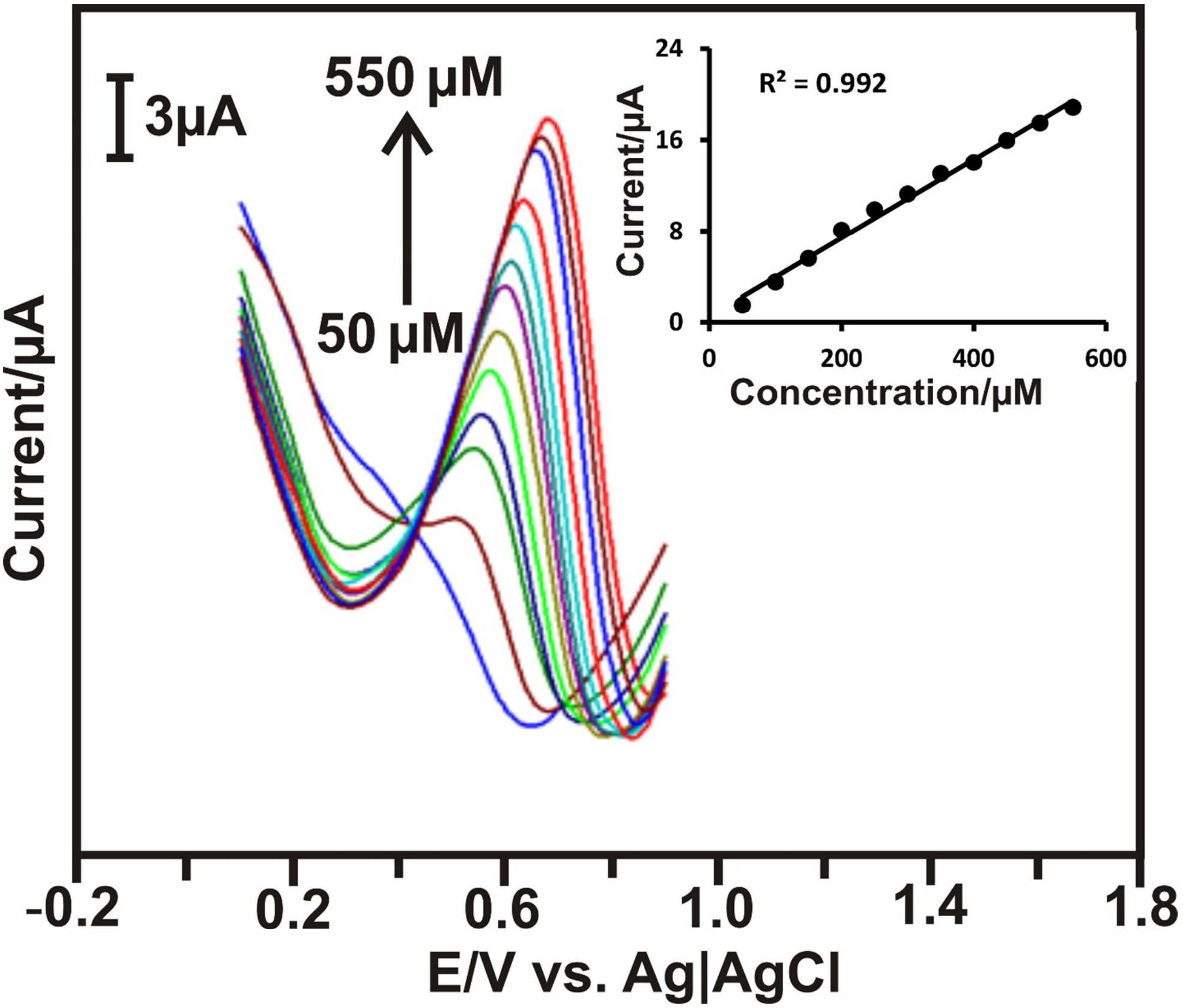
3μA
550 μM
50 μM
Current/μA
-0.2
0.2
0.6
1.0
1.4
1.8
E/V vs. Ag|AgCl
R² = 0.992
24
16
8
0
Current/μA
0
200
400
600
Concentration/μM